Solution rheology of mesquite gum in comparison with gum arabic

F.M. Goycoolea,[a] E.R. Morris,[a]* R.K. Richardson[a] & A.E. Bell[b]

[a]*Department of Food Research and Technology, Cranfield University, Silsoe College, Silsoe, Bedford MK45 4DT, UK*
[b]*Department of Food Science and Technology, Reading University, Whiteknights, Reading RG6 2AP, UK*

Commercial samples of mesquite gum and food-grade gum arabic were purified by filtration, alcohol precipitation, and extensive dialysis, and their rheological properties were characterised over the full range of concentrations at which solutions could be prepared (up to ~50% w/w). Both gave typical solution-like mechanical spectra, with close Cox–Merz superposition of $\eta(\dot{\gamma})$ and $\eta^*(\omega)$ and only slight shear thinning at the highest accessible concentrations, and $(\ln \eta_{rel})/c$ varied linearly with log c from below 2% w/w to above 50%. The intrinsic viscosity of mesquite gum ($[\eta] \approx 0{\cdot}11$ dl g^{-1}) was appreciably lower than that of gum arabic ($[\eta] \approx 0{\cdot}19$ dl g^{-1} in 0·1 M NaCl at 20°C), and was independent of ionic strength above $I \approx 0{\cdot}05$, indicating a compact structure capable of only limited contraction. Departures from dilute-solution behaviour ($\eta \sim c^{1{\cdot}4}$) occurred at $c[\eta] \approx 1$ for both materials, with a progressive increase in concentration dependence at higher space-occupancy, behaviour typical of soft, deformable particles, rather than of interpenetrating macromolecules. The increase in viscosity with increasing concentration was steeper for mesquite, consistent with evidence from size-exclusion chromatography and dynamic light scattering that the larger (and presumably more deformable) 'wattle blossom' component of gum arabic was absent from the mesquite gum sample.

INTRODUCTION

Mesquite gum is produced by the nitrogen-fixing desert shrub *Prosopis* (Greenwood & Morey, 1979), from the same botanical family as the *Acacia* species which yield gum arabic. Several species of *Prosopis* grow wild in the Sonorean desert of northwestern Mexico, and the gum is collected by hand, in very much the same way as gum arabic, providing a source of income to rural families. Mesquite gum is used in domestic cooking in the Sonora region, to prepare a traditional dessert known as 'capirotada', but approval as a commercial food additive is unlikely, because of the high content of tannic compounds (Anderson & Weiping, 1989). The main current uses are in the ink, textile and glue industries. In view of the rising cost of gum arabic, coupled with limitations and variability of supply (Gordon & Krishnakumar, 1990; Whistler, 1993), mesquite gum may become an increasingly important alternative in such non-food applications (Saunders & Becker, 1989).

The two materials show striking similarities in primary structure. Both appear to have a 'core' of β-D-galactose residues, comprising a (1→3)-linked backbone with (1→6)-linked branches, bearing L-arabinose (pyranose and furanose ring forms), L-rhamnose, β-D-glucuronate and 4-*O*-methyl-β-D-glucuronate as single sugar or oligosaccharide side chains (see Aspinall & Whitehead, 1970*a*, 1970*b*; Churms *et al.*, 1981; Anderson & Farquhar, 1982 for mesquite; Street & Anderson, 1983; Churms *et al.*, 1983; Defaye & Wong, 1986 for gum arabic). Recent work, however, indicates that the two gums may be distinguished by antibodies specific to different non-reducing chain termini (Miskiel & Pazur, 1991).

In addition to the carbohydrate constituents, gum arabic contains ~2·4% protein (Anderson & Stoddart, 1966; Osman *et al.*, 1993*a*). As well as having a crucial role in emulsification (Randall *et al.*, 1988; Dickinson *et al.*, 1991*a*, 1991*b*), it is now evident that the protein component is central to the overall primary structure. Gum arabic can be separated into two principal fractions. The main fraction (fraction 1), whose contribution to the total has been reported as ~70% by Vandevelde and Fenyo (1985) and ~88% by Randall *et al.* (1989), has a lower protein content than the unfractionated gum (<0·5%) and an average molecular mass

*To whom correspondence should be addressed.

of $\sim 2{\cdot}8 \times 10^5$, which does not change significantly on extensive proteolysis. The smaller fraction (fraction 2) has a much higher protein content (~12%) and an average molecular mass about 5 times that of the major fraction ($\sim 14{\cdot}5 \times 10^5$). On proteolysis, the molecular mass of fraction 2 drops to that of fraction 1 (Connolly *et al.*, 1987, 1988; Randall *et al.*, 1989), suggesting a 'wattle blossom' structure with, on average, five branched carbohydrate assemblies similar, or identical, to those in fraction 1, linked together by a polypeptide chain. No such investigations have yet been reported for mesquite gum, but it has a protein content comparable to that of gum arabic (Anderson & Farquhar, 1982; Jurasek & Phillips, 1993).

Recent studies have shown that the major fractions of gum arabic may contain subfractions with subtle differences in primary structure (Osman *et al.*, 1993*a*, 1993*b*). There is also a minor (~1·5%) 'glycoprotein' component which contains about 25% of the total protein (Randall *et al.*, 1989), and may again consist of discrete subfractions. The overall composition of the gum varies significantly between *Acacia* species, and the precise definition of 'gum arabic', particularly for food use, is under review (FAO, 1990). There is comparable variation in the composition of exudate gums from *Prosopis* (Anderson & Farquhar, 1982), and commercial 'mesquite gum' normally contains material from several different species.

Because of its highly branched, compact structure, gum arabic gives much lower viscosity, and can be dissolved to much higher concentrations, than most other hydrocolloids of comparable molecular weight. The purpose of the present investigation was to compare the rheology of mesquite gum with that of gum arabic over the full range of concentrations at which solutions could be prepared, and to explore the relationships between molecular structure and solution properties.

MATERIALS AND METHODS

Gum samples

A typical sample of commercial mesquite gum was purchased from a local retail outlet in Hermonsillo, Mexico. Food-grade gum arabic was supplied by Thew Arnott Ltd, Wallingford, Surrey, UK. The 'tears' of crude gum were dissolved in water, and any course debris present was removed by passing the solutions through muslin. The polysaccharide was then precipitated with ethanol and redissolved. The resulting solutions were clarified by filtration (Whatman No. 4 filter paper), dialysed for 48 h against four changes of distilled deionised water, and freeze-dried. Distilled deionised water was used in all subsequent experiments, and all chemicals were of analytical grade from BDH.

The freeze-dried samples were analysed for tannins by the procedure of Anderson and Morrison (1989). Gum solutions were prepared at 2% w/w, and 10 ml aliquots were reacted at room temperature with 0·1 ml of freshly prepared ferric chloride reagent (9 g $FeCl{\cdot}6H_2O$ made up to 100 ml with water). The tannin content was then determined by measurement of absorption at 430 nm on a Pye-Unicam 8620 spectrophotometer, using tannic acid for calibration. No tannin was detected in the gum arabic sample, as expected for food-grade material. The value obtained for the sample of mesquite gum was 0·60%, somewhat lower than those reported previously (Anderson & Weiping, 1989) for other *Prosopis* exudates (0·7–3·4%). The mesquite sample was tested further by boiling ~50 mg of the gum for 30 min in 5 ml of 2 M HCl; the red colouration characteristic of condensed tannins was not observed, indicating that only simple tannins were present.

Specific optical rotation at 589 nm ($[\alpha]_D$) was measured at 20°C using a Perkin-Elmer 241 polarimeter (polymer concentration 0·5% w/w; pathlength 10 cm). The gum arabic sample gave $[\alpha]_D = -32$, within the range typical of food-grade *Acacia* gums (Jurasek & Phillips, 1993). As found for other *Prosopis* gums (with the exception of the exudate from *P. juliflora*), the mesquite gum gave a positive optical rotation, but the absolute value obtained, $[\alpha]_D = 54$, was somewhat lower than those reported previously (61–88; Anderson & Farquhar, 1982).

Preparation of solutions of known ionic strength

Since mesquite gum and gum arabic both contain charged residues (glucuronate and 4-*O*-methyl glucuronate), the ionic strength of solutions prepared in distilled water will vary with polymer concentration. The following procedure was, therefore, adopted to allow results to be compared under known, fixed concentrations of ionic strength. Solutions were prepared at the highest possible polymer concentration, by allowing the freeze-dried gums to hydrate slowly (overnight) in the minimum volume of water necessary to give a clear solution. The resulting solutions were homogenised using a vortex mixer and dialysed to equilibrium against three changes of the required concentration of NaCl, and the final dialysate was used for all subsequent dilutions. In calculating the concentration of the stock solution, correction was made for changes in volume during dialysis, by weighing the sample at the beginning and end of the dialysis procedure. Where necessary, stock solutions were prepared at lower initial concentration, to allow measurements to be made at ionic strengths below those generated by the counterions to the polymer in very concentrated solutions.

Investigation of molecular size

Solutions of mesquite gum dialysed against 5, 10, 25 and 50 mM NaCl were prepared at concentrations of ~5·0, 2·5 and 1·0 mg ml^{-1} and filtered to optical clarity

through Millipore membranes of pore sizes 0·45 and 0·22 μm. The translational diffusion coefficient of the polymer in each solution was then determined by dynamic light scattering (780 nm wavelength; 90° scattering angle) using an M801 molecular size detector from Oros Instruments Ltd, Slough, UK.

The same instrument was used in conjunction with a size-exclusion gel chromatography column (Sepharose CL-4B-200; Sigma Chemicals) to monitor the distribution of molecular size. A solution of mesquite gum (5·5 mg ml^{-1}) in 2 M NaCl was clarified as described above and eluted with phosphate buffer (pH 6·55; 50 mM NaCl), using a peristaltic pump to control the flow rate. The eluate was passed through a 0·1 μm filter (Anotec) into the inlet port of the molecular size detector, with the intensity of scattering giving an index of concentration and the diffusion coefficient giving a measure of molecular size (hydrodynamic radius). The same technique has been applied to samples of gum arabic by White *et al.* (1992), and their paper gives a fuller account of the principles and operation of the Oros detector.

Rheological studies

All rheological measurements were made at 20°C. Dilute solution viscosity was measured on a Contraves Low Shear 30 rotational viscometer, using cup-and-bob geometry with inner and outer radii of 5·5 and 6·0 mm, respectively. Solutions of higher viscosity were measured on a Sangamo Viscoelastic Analyser, using cone-and-plate geometry of diameter 5 cm and cone angle 2°. Low-amplitude oscillatory measurements of storage modulus (G'), loss modulus (G'') and complex dynamic viscosity (η^*) over the frequency range 0·1–100 rad s^{-1} were made using cone-and-plate geometry (5 cm diameter; 0·05 rad cone angle) on a sensitive prototype rheometer designed and constructed by one of us (R.K.R.).

RESULTS

Dynamic light scattering

Figure 1 shows the variation of translational diffusion coefficient (D_t) with salt concentration for mesquite gum at 0·1, 0·25 and 0·5% w/w. Because of the complex and incompletely characterised primary structure of mesquite gum, the quantitative analyses developed for linear polyelectrolytes (see for example Magdelenat *et al.*, 1981) cannot be applied, but the results are qualitatively similar. In particular, the reduction in D_t with increasing salt is an expected consequence of electroviscous interactions between the polyanion and the surrounding simple cations.

As shown in Fig. 2, there is an approximately linear reduction in D_t for mesquite gum with decreasing ratio

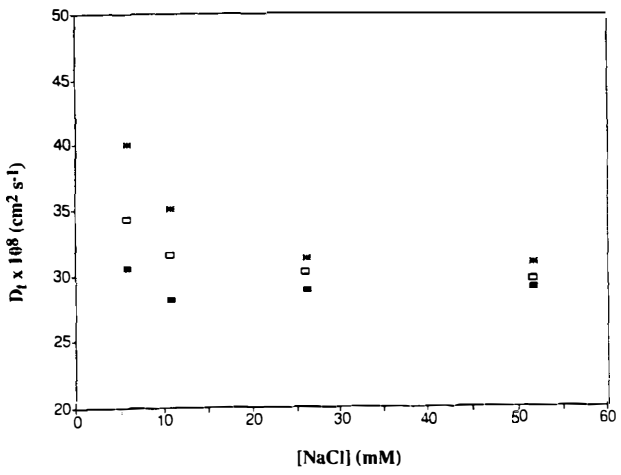

Fig. 1. Variation of translational diffusion coefficient (D_t) with salt (NaCl) concentration for mesquite gum at polymer concentrations (% w/w) of 0·10 (■), 0·25 (□) and 0·50 (*). Measurements were made at ~26·8°C (300 K).

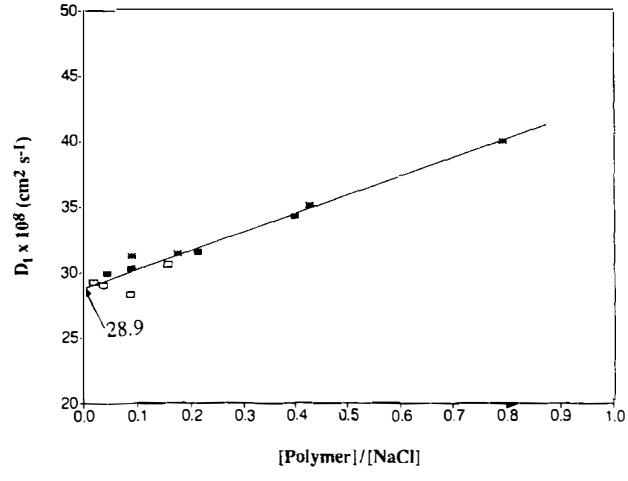

Fig. 2. Diffusion coefficients from Fig. 1, plotted as a function of the molar ratio of the concentration of negatively charged groups on mesquite gum to the concentration of surrounding cations. Symbols as in Fig. 1.

of polymer to counterion (Na^+), giving an intercept of $D_t \approx 28{\cdot}9 \times 10^8$ cm^2 s^{-1} at infinite ionic strength and/or at infinite dilution. The corresponding mean hydrodynamic radius (R_h) was determined by the Stokes–Einstein equation:

$$R_h = kT/6\pi\eta D_t, \quad (1)$$

where k is the Boltzmann constant (1·381 × 10^{-23} J K^{-1}), and η is the viscosity of the solvent (~0·85 mPa s for water at 300 K, the temperature at which the measurements were made). As shown in Table 1, the value obtained (R_h = 8·5 nm) is close to that reported for the protease-insensitive 'fraction 1' of gum arabic (Randall *et al.*, 1989), but substantially lower than the corresponding values for whole gum arabic or for the 'wattle blossom' assembly (fraction 2).

Size distribution

Figure 3 shows the elution profile obtained for mesquite gum by size-exclusion chromatography, as characterised by the 'count rate' from the light-scattering detector, and by the accompanying changes in hydrodynamic radius (White *et al.*, 1992). The observed values of R_h are confined to a rather narrow range (~8·2–10·6 nm), spanning the mean value of R_h = 9·2 nm reported for fraction 1 of gum arabic (Randall *et al.*, 1989). The variation of scattering intensity with elution volume, however, indicates the presence of at least two subfractions, perhaps analogous to fractions 1A and 1B observed in hydrophobic affinity chromatography of gum arabic (Osman *et al.*, 1993*a*).

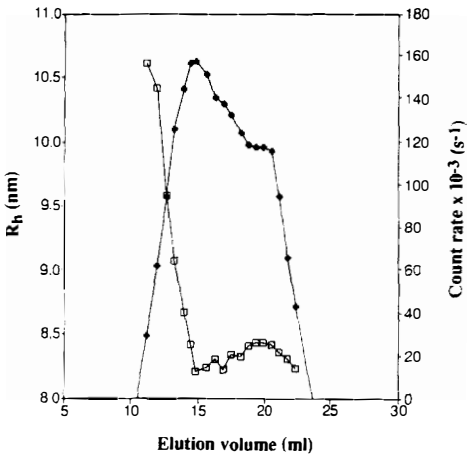

Fig. 3. Elution profile for mesquite gum on Sepharose CL-4B-200. Polymer concentration is characterised by the count rate (+) and molecular size by the hydrodynamic radius, R_h (□). Measurements were made at 300 K.

Intrinsic viscosity

The intrinsic viscosity, $[\eta]$, of the two gum samples (at 25°C in 0·1 M NaCl) was determined from experimental measurements of Newtonian viscosity at low shear rate by the following standard relationships (see Bohdanecký & Kovár, 1982).

$$\eta_{rel} = \eta/\eta_s \quad (2)$$

$$\eta_{sp} = (\eta - \eta_s)/\eta_s = \eta_{rel} - 1 \quad (3)$$

$$\eta_{sp}/c = [\eta] + k'[\eta]^2 c \quad (4)$$

$$(\ln \eta_{rel})/c = [\eta] + k''[\eta]^2 c \quad (5)$$

$$[\eta] = \{2(\eta_{sp} - \ln \eta_{rel})\}^{1/2}/c, \quad (6)$$

where η and η_s are the viscosities of the solution and the solvent, respectively, η_{rel} and η_{sp} are the (dimensionless) parameters of relative and specific viscosity, c is concentration and k′ and k″ are constants. Equations 4, 5 and 6 are known, respectively, as the Huggins, Kraemer and 'single point' relationships. As shown in Fig. 4, all three relationships gave reasonably linear extrapolations to infinite dilution for both samples, with satisfactory convergence to a common intercept ($[\eta]$) at $c = 0$. The intrinsic viscosity obtained for mesquite gum (Fig. 4a) was substantially lower than that of gum arabic (Fig. 4b), consistent with the smaller hydrodynamic radius from light scattering (Table 1).

The intrinsic viscosity of polyelectrolytes normally decreases with increasing ionic strength (I), due to progressive shielding of intramolecular electrostatic repulsions allowing the molecules to contract to a less expanded conformation. Quantitatively, $[\eta]$ decreases linearly with $I^{-1/2}$, and the slope gives an index of chain flexibility (Smidsrød & Haug, 1971). However, as shown in Fig. 5, there was no systematic change in the intrinsic viscosity of mesquite gum at ionic strengths ranging from 0·05 to 2·0, with $[\eta]$ remaining essentially constant at ~0·11 ± 0·01 dl g^{-1}.

The lower limit of the range of ionic strengths studied was imposed by the concentration of polymer needed to

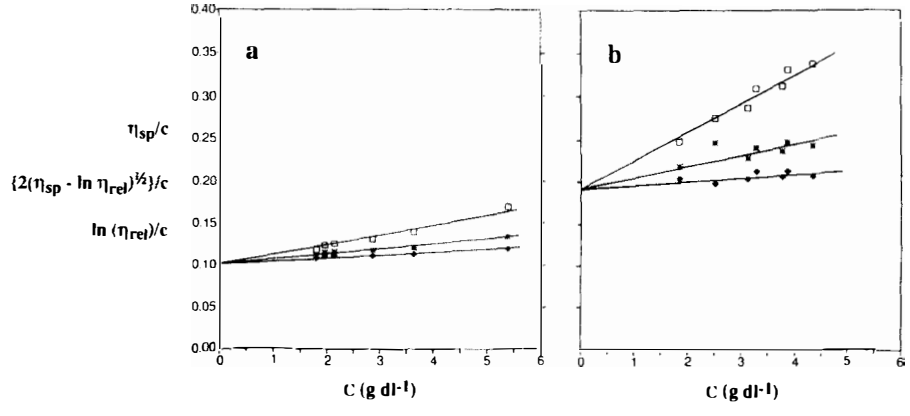

Fig. 4. Determination of intrinsic viscosity (20°C; 0·1 M NaCl) for: (a) mesquite gum; and (b) gum arabic by combined Huggins (□), Kraemer (+) and single-point (∗) extrapolation of, respectively, η_{sp}/c, $(\ln \eta_{rel})/c$ and $\{2(\eta_{sp} - \ln \eta_{rel})\}^{1/2}/c$ to zero concentration.

Table 1. Hydrodynamic radius, R_h, and intrinsic viscosity, $[\eta]$, for exudate gums

Material	R_h (nm)	$[\eta]$ (dl g^{-1})[a]
Mesquite gum	8·5	0·11[b]
Gum arabic		
'whole' gum	14·1[c]	0·19
fraction 1	9·2[c]	—
fraction 2	22·8[c]	—

[a]At 20°C in 0·1 M NaCl.
[b]Mean value from Fig. 5.
[c]From Randall *et al.* (1989).

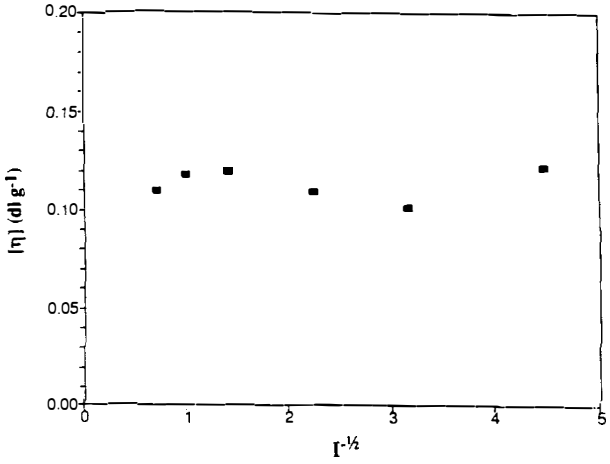

Fig. 5. Variation of intrinsic viscosity (20°C) with ionic strength (I) for mesquite gum dialysed to equilibrium against NaCl solutions with concentrations ranging from 0·05 to 2·0 M.

give relative viscosities between ~1·2 and 2·0, as required for reasonable linearity and precision in extrapolation to infinite dilution (Morris, 1984). As indicated in Fig. 4a, the appropriate range of concentrations extends to ~5·5% w/w. The equivalent weight (i.e. molecular mass per charge) for mesquite gum is ~1075 (Anderson & Farquhar, 1982), so that 5·5% corresponds to ~50 mM (i.e. to $I \approx 0{\cdot}05$ with Na^+ as counterion). However, some indication of the behaviour at lower ionic strength was obtained by direct comparison of the viscosity of dilute solutions (2% w/v) of mesquite gum in water and at the NaCl concentrations used for determinations of $[\eta]$ (Fig. 5). As shown in Fig. 6, the specific viscosity in water (where the concentration of counterions to the polymer is ~18·6 mM) was about three times higher than the values obtained at Na^+ concentrations of 50 mM or above. Although the higher viscosity in water may be due, in part, to electrical double-layer effects, the magnitude of the change suggests that the structure of mesquite gum is capable of substantial expansion at low ionic strength, but collapses to a compact form resistant to further spontaneous contraction at, or below, ~50 mM salt.

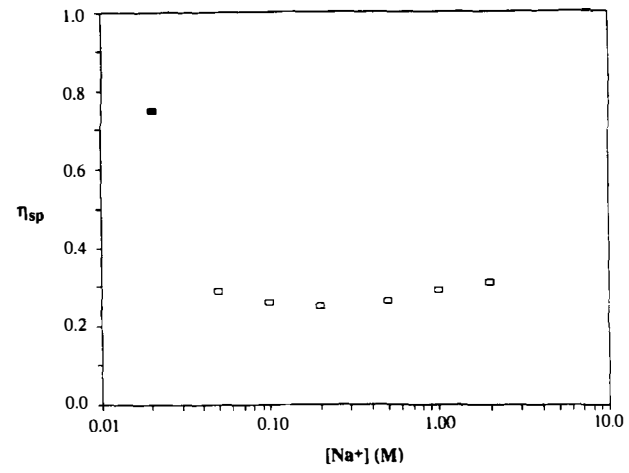

Fig. 6. Variation of specific viscosity (20°C) with cation (Na^+) concentration for mesquite gum (2% w/w) in water (■) and after dialysis against 0·05, 0·1, 0·2, 0·5, 1·0 and 2·0 M NaCl (□).

Concentrated-solution rheology

Both gum samples could be dissolved to concentrations of at least 50% w/w. As shown in Fig. 7, the mechanical spectra obtained for these extremely concentrated preparations were similar to those seen for typical linear polysaccharides at much lower concentrations (see, for example, Ross-Murphy, 1984). Viscous flow (loss modulus, G'') predominates over elastic response (storage modulus, G') throughout the accessible frequency range, both moduli increase steeply with increasing frequency, but the dynamic viscosity (η^*) is virtually Newtonian (i.e. independent of frequency).

A further point of similarity to the behaviour of normal solutions of disordered linear chains is that both of the exudate gums obey the Cox–Merz rule (Cox & Merz, 1958): steady-shear viscosity (η) and complex dynamic viscosity (η^*) superimpose closely (Fig. 7) at equivalent values of shear rate ($\dot{\gamma}/s^{-1}$) and frequency (ω/rad s^{-1}). Departures from Cox–Merz superposition occur for networks held together by bonding interactions that are broken down by steady shear but that survive low-amplitude oscillatory deformation (giving $\eta < \eta^*$); the absence of any such departures indicates that the intermolecular interactions in solutions of mesquite gum (Fig. 7a) or gum arabic (Fig. 7b) are topological rather than enthalpic.

In a previous study of the rheology of mesquite gum, substantial 'shear thickening' (i.e. increase in η with increasing $\dot{\gamma}$) was observed for comparatively dilute solutions (1–20% w/v) at shear rates above ~100 s^{-1}. The authors (Vernon Carter & Sherman, 1980) attributed this effect to either a change in molecular shape at high shear rates, or an experimental artefact caused by turbulent flow in the coaxial cylinder geometry used. As illustrated in Fig. 8, the values

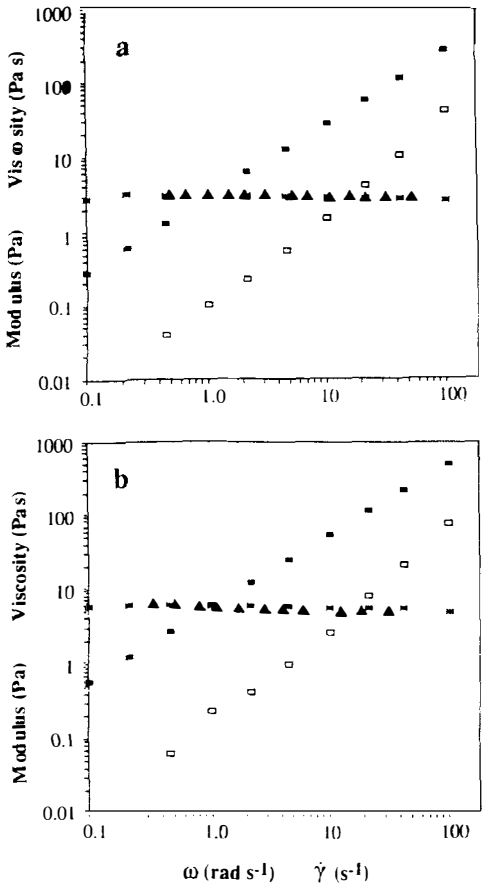

Fig. 7. Mechanical spectra (20°C; 0·1 M NaCl) for 50% w/w solutions of: (a) mesquite gum; and (b) gum arabic, showing the variation of G' (□), G'' (■) and η^*(∗) with frequency (ω). The dependence of steady shear viscosity (η) on shear rate ($\dot{\gamma}$) is also shown (▲).

obtained in the present work, using cone-and-plate geometry, gave no indication of any such behaviour, even at very much higher concentrations of polymer. Instead, slight shear thinning was observed at concentrations above ~20% w/w, and at lower concentrations the solutions became Newtonian (η independent of $\dot{\gamma}$).

The form of shear thinning was different from that typical of entangled linear polysaccharides (Morris, 1990), with no indication of an increase in the slope (S) of log η vs log $\dot{\gamma}$ with increasing shear rate, or of a 'Newtonian plateau' at low rates. As shown in Fig. 8, the decrease in log η with increasing log $\dot{\gamma}$ was essentially linear, and could therefore be fitted to a 'power law' relationship:

$$\log \eta = \log k + S \log \dot{\gamma} \tag{7}$$

$$\text{i.e.} \quad \eta = k \dot{\gamma}^S, \tag{8}$$

where k is the viscosity at $\dot{\gamma} = 1\ s^{-1}$ (i.e. at log $\dot{\gamma} = 0$). Concentrated solutions of gum arabic showed similar behaviour.

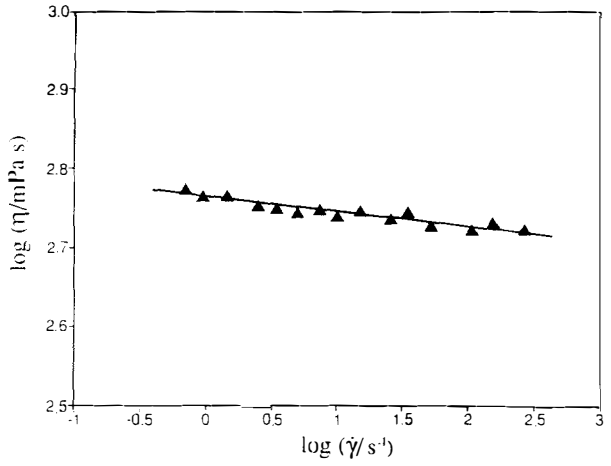

Fig. 8. Shear rate ($\dot{\gamma}$) dependence of viscosity (η) for mesquite gum (40% w/w; 0·1 M NaCl; 20°C).

Concentration-dependence of viscosity

Most linear polysaccharides show an essentially identical variation of solution viscosity (measured at low shear rate, before the onset of shear thinning) with degree of space-occupancy, as characterised by the (dimensionless) product of concentration (proportional to the number of coils present) and intrinsic viscosity (proportional to the volume occupied by each coil). Double logarithmic plots of η_{sp} vs $c[\eta]$ for different polysaccharides, or for the same polysaccharide at different molecular weights, superimpose closely, and show a sharp change of slope from ~1·4 to ~3·3 at $\eta_{sp} \approx 10$ and $c[\eta] \approx 4$ (Morris *et al.*, 1981). The 'breakpoint' marks the transition from a solution of chains free to move independently to an entangled network. Initial contact (i.e. complete space-occupancy by the individual coils, prior to the onset of interpenetration), however, occurs earlier, at $c[\eta] \approx 1$, and can be detected by, for example, measurements of self-diffusion rates from dynamic light scattering (e.g. Southwick *et al.*, 1979) or fluorescence bleaching (e.g. Tinland *et al.*, 1990).

Figure 9 shows analogous plots of log η_{sp} vs log $c[\eta]$ for mesquite gum and gum arabic (in 0·1 M NaCl at 20°C), in direct comparison with the behaviour typical of disordered linear chains. As discussed above, concentrated solutions of the exudate gums do not give an accessible Newtonian plateau at low shear rate, and the viscosity at 1 s^{-1} (k in equations (7) and (8)) was substituted for the 'zero shear' value (η_0) used in characterisation of linear polysaccharides (Morris *et al.*, 1981). However, since the extent of shear thinning is slight (Fig. 8) this difference should have little effect on the comparison.

At low degrees of space-occupancy, all three plots coincide closely, but the exudate gums show departure from the common slope of ~1·4 at $c[\eta] \approx 1$ (i.e. on

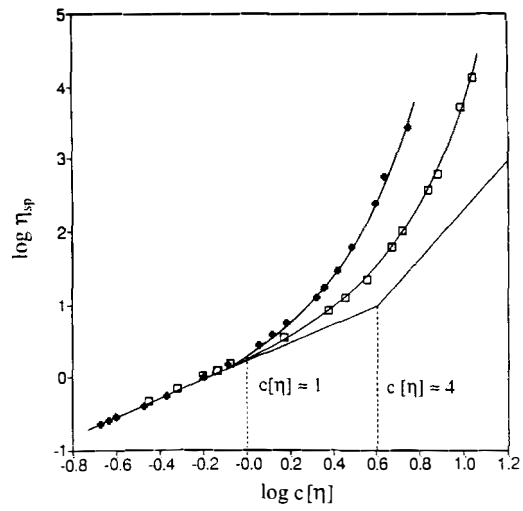

Fig. 9. Variation of specific viscosity (η_{sp}) with space occupancy (c[η]) for mesquite gum (+) and gum arabic (□) at 20°C in 0·1 M NaCl. The third trace (without symbols) shows the behaviour typical of disordered linear polysaccharides (Morris *et al.*, 1981).

initial contact), with a steady increase in slope at higher concentrations, in contrast to the sharp break and subsequent linearity seen for entangled coils. The increase in viscosity with increasing concentration above $c[\eta] \approx 1$ is much greater for mesquite gum than for gum arabic, suggesting a more compact structure with greater resistance to interpenetration. Indeed, when measured viscosities are plotted against absolute concentration (Fig. 10), rather than against $c[\eta]$, the values for mesquite gum converge with those for gum arabic at concentrations above ~35% w/w, despite its much lower hydrodynamic volume (Table 1).

A peculiar feature observed for both materials is that the parameter $(\ln \eta_{rel})/c$ used in the Kraemer extrapolation to intrinsic viscosity (equation (5)) shows a virtually linear dependence on log c (Fig. 11) throughout the concentration-range studied (from below 2% w/w to above 50%). Although entirely empirical, this behaviour allows the viscosity of the exudate gums to be expressed, with reasonable precision, as a simple function of concentration. The slopes of the linear plots of Fig. 11 are 0·0369 for mesquite gum and −0·0356 for gum arabic, and the corresponding intercepts at log $c = 0$ (i.e. at $c = 1\%$ w/w) are 0·091 and 0·221, respectively, yielding the following relationships:

$$\text{mesquite:} \quad \eta_{rel} = \text{EXP}\{c(0{\cdot}091 + 0{\cdot}0369 \log c)\} \qquad (9)$$

$$\text{arabic:} \quad \eta_{rel} = \text{EXP}\{c(0{\cdot}221 - 0{\cdot}0356 \log c)\}, \qquad (10)$$

with c expressed in % w/w. At 20°C (the temperature at which the measurements were made), the viscosity of water (i.e. η_s in equation (2)) is 1 mPa s. Thus the values of η_{rel} derived from equations (9) and (10) are numerically identical to the absolute viscosity at that temperature (also expressed in mPa s).

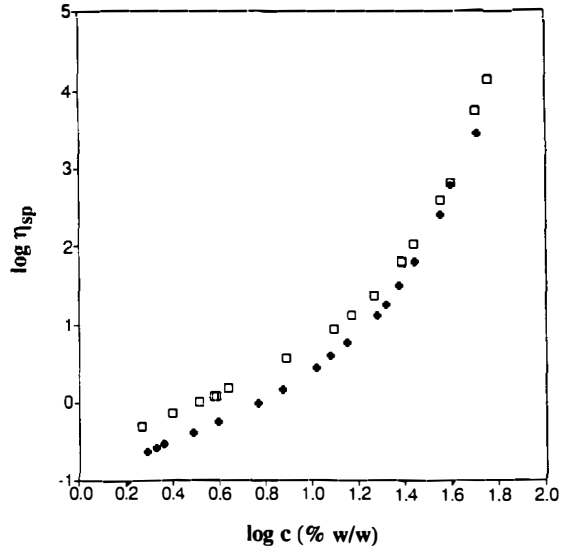

Fig. 10. Concentration dependence of specific viscosity (20°C; 0·1 M NaCl) for mesquite gum (+) and gum arabic (□).

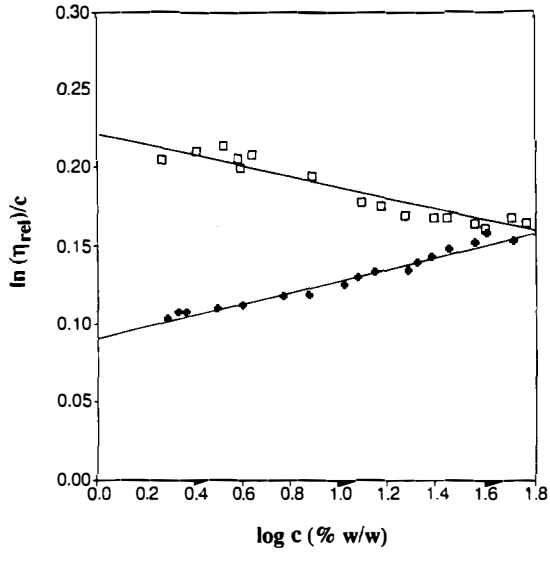

Fig. 11. Concentration dependence of $(\ln \eta_{rel})/c$ for mesquite gum (+) and gum arabic (□) at 20°C in 0·1 M NaCl.

DISCUSSION AND CONCLUSIONS

As might be expected from their known similarity of primary structure, mesquite gum and gum arabic show some striking similarities in solution properties. High concentrations (50% w/w) of both materials give typical solution-like mechanical spectra (Fig. 7) similar to those of comparatively dilute solutions of disordered linear polysaccharides. Both give close Cox–Merz superposition of $\eta(\dot{\gamma})$ and $\eta^*(\omega)$, consistent with only topological interactions between individual molecules.

Both show departure from dilute-solution viscosity (Fig. 9) on initial contact (at $c[\eta] \approx 1$) rather than at the higher degree of space-occupancy typical of linear chains ($c[\eta] \approx 4$), as would be expected for densely branched structures with little scope for mutual interpenetration. At higher concentrations (above $c[\eta] \approx 1$), there is a progressive increase in the concentration dependence of viscosity for both materials (Fig. 9), as found for 'microgel' particles (e.g. Carnali & Naser, 1992) and similar 'soft spheres' (Everett, 1988), rather than the $c^{3.3}$ dependence observed (Morris *et al.*, 1981) for interpenetrating coils.

The absence of significant interpenetration and entanglement is also evident in the very limited shear thinning (Fig. 8) seen for concentrated solutions of the exudate gums, in marked contrast to the behaviour of entangled networks of linear polysaccharides, which show large reductions in viscosity when the rate of forced disentanglement exceeds the rate at which new entanglements can form between different chain partners. It would, therefore, appear that the individual molecules of mesquite gum or gum arabic in concentrated solutions are squashed together like balls of foam rubber crammed into a jar, rather than interpenetrating like coils of wire. The increase in viscosity with increasing concentration above $c[\eta] \approx 1$, however, is much steeper for mesquite gum than for gum arabic (Fig. 9), indicating a more compact structure with greater resistance to forced contraction. The response of mesquite gum to changes in salt concentration in dilute solution (Figs 5 and 6) is also consistent with a densely packed structure which can be expanded by intramolecular electrostatic repulsion at low ionic strength (Fig. 6), but which has only limited scope for contraction at higher salt.

A likely explanation is that, as indicated by the hydrodynamic data presented in Table 1, mesquite gum (or, more strictly, the commercial sample used in the present work, after clarification, alcohol precipitation, and extensive dialysis) has a structure similar to the 'monomeric' fraction 1 of gum arabic, with few, if any, 'wattle blossom' assemblies analogous to those in fraction 2. Although fraction 2 constitutes only ~10% of the total mass of gum arabic (Randall *et al.*, 1989), it will make a disproportionate contribution to the solution rheology, because of its much larger hydrodynamic volume. It seems reasonable to suppose that molecules consisting of several (typically five) dense carbohydrate 'globules' linked through a polypeptide chain would have a more open, flexible structure than the individual 'globules' in isolation, and would, therefore, be less resistant to contraction in response to increasing concentration. If this interpretation is correct, it would follow that proteolysis of gum arabic, to dissociate the 'wattle blossom' structure, should yield solution properties (including, in particular, the concentration dependence of viscosity) closely similar to those documented here for mesquite gum, a conclusion which could be tested experimentally.

ACKNOWLEDGEMENTS

We thank Dr D.M.W. Anderson (Edinburgh University, Dr P.A. Williams (North East Wales Institute) and Professor S.B. Ross-Murphy (Kings College, London) for advice and discussions, and Professor L. Pyle for generous access to the Oros molecular size detector. We also thank The British Council and CONACYT (Mexico) for studentship support to one of us (F.M.G.)

REFERENCES

Anderson, D.M.W. & Farquhar, J.G.K. (1982). *Int. Tree Crops J.*, **2,** 15–24.

Anderson, D.M.W. & Morrison, N.A. (1989). *Food Hydrocolloids*, **3,** 57–63.

Anderson, D.M.W. & Stoddart, J.F. (1966). *Carbohydr. Res.*, **2,** 104–14.

Anderson, D.M.W. & Weiping, W. (1989). *Food Hydrocolloids*, **3,** 235–42.

Aspinall, G.O. & Whitehead, C.C. (1970*a*). *Can. J. Chem.*, **48,** 3840–9.

Aspinall, G.O. & Whitehead, C.C. (1970*b*). *Can. J. Chem.*, **48,** 3850–5.

Bohdanecký, M. & Kovár, J. (1982). *Viscosity of Polymer Solutions*. Elsevier, Amsterdam, The Netherlands.

Carnali, J.O. & Naser, M.S. (1992). *Colloid Polym. Sci.*, **270,** 183–93.

Churms, S.C., Merrifield, E.H. & Stephen, A.M. (1981). *Carbohydr. Res.*, **90,** 261–7.

Churms, S.C., Merrifield, E.H. & Stephen, A.M. (1983). *Carbohydr. Res.*, **123,** 267–79.

Connolly, S., Fenyo, J.C. & Vandevelde, M.C. (1987). *Food Hydrocolloids*, **1,** 477–80.

Connolly, S., Fenyo, J.C. & Vandevelde, M.C. (1988). *Carbohydr. Polym.*, **8,** 23–32.

Cox, W.P. & Merz, E.H. (1958). *J. Polym. Sci.*, **28,** 619–22.

Defaye, J. & Wong, E. (1986). *Carbohydr. Res.*, **150,** 221–31.

Dickinson, E., Galazka, V.B. & Anderson, D.M.W. (1991*a*). *Carbohydr. Polym.*, **14,** 373–83.

Dickinson, E., Galazka, V.B. & Anderson, D.M.W. (1991*b*). *Carbohydr. Polym.*, **14,** 385–92.

Everett, D.H. (1988). *Basic Principles of Colloid Science*. Royal Society of Chemistry, Cambridge, UK.

FAO (1990). *Specifications for Identity and Purity of Certain Food Additives*. Food and Nutrition Paper 49, Food and Agriculture Organisation of the United Nations, Rome, Italy, pp. 23–5.

Gordon, I.R. & Krishnakumar, V. (1990). *Int. Food Ingredients*, **3,** 30–3.

Greenwood, C. & Morey, P. (1979). *Bot. Gaz.*, **140,** 32–8.

Jurasek, P. & Phillips, G.O. (1993). *Food Hydrocolloids*, **7,** 337–52.

Magdelenat, H., Turq, P., Tivant, P. & Drifford, M. (1981). In *Solution Properties of Polysaccharides*, ed. D. Brant. American Chemical Society, Washington DC, USA, pp. 387–403.

Miskiel, F.J. & Pazur, J.H. (1991). *Carbohydr. Polym.*, **16,** 17–35.

Morris, E.R. (1984). In *Gums and Stabilisers for the Food Industry 2*, eds G.O. Phillips, D.J. Wedlock & P.A. Williams. Pergamon Press, Oxford, UK, pp. 57–78.
Morris, E.R. (1990). *Carbohydr. Polym.*, **13,** 85–96.
Morris, E.R., Cutler, A.N., Ross-Murphy, S.B., Rees, D.A. & Price, J. (1981). *Carbohydr. Polym.*, **1,** 5–21.
Osman, M.E., Menzies, A.R., Williams, P.A., Phillips, G.O. & Baldwin, T.C. (1993*a*). *Carbohydr. Res.*, **246,** 303–18.
Osman, M.E., Williams, P.A., Menzies, A.R. & Phillips, G.O. (1993*b*). *J. Agric. Food Chem.*, **41,** 71–7.
Randall, R.C., Phillips, G.O. & Williams, P.A. (1988). *Food Hydrocolloids*, **2,** 131–40.
Randall, R.C., Phillips, G.O. & Williams, P.A. (1989). *Food Hydrocolloids*, **3,** 65–75.
Ross-Murphy, S.B. (1984). In *Biophysical Methods in Food Research*, ed. H.W.-S. Chan. Critical Reports on Applied Chemistry, Vol. 5, SCI, London, UK, pp. 138–99.
Saunders, R.M. & Becker, R. (1989). In *New Crops for Food and Industry*, eds G.E. Wickens, N. Haq & P. Day. Chapman and Hall, London, UK, pp. 288–302.
Smidsrød, O. & Haug, A. (1971). *Biopolymers*, **10,** 1213–27.
Southwick, J.G., McDonnell, M.E., Jamieson, A.M. & Blackwell, J. (1979). *Macromolecules*, **12,** 305–11.
Street, C.A. & Anderson, D.M.W. (1983). *Talanta*, **30,** 887–93.
Tinland, B., Maret, G. & Rinaudo, M. (1990). *Macromolecules*, **23,** 596–602.
Vandevelde, M.C. & Fenyo, J.C. (1985). *Carbohydr. Polym.*, **5,** 251–93.
Vernon Carter, E.J. & Sherman, P. (1980). *J. Text. Stud.*, **11,** 339–49.
Whistler, R.L. (1993). In *Industrial Gums: Polysaccharides and Their Derivatives*, eds R.L. Whistler & J.N. BeMiller, 3rd edition. Academic Press, San Diego, CA, USA, pp. 309–39.
White, R., Anderson, D.M.W. & Claes, P. (1992). In *Gums and Stabilisers for the Food Industry 6*, eds G.O. Phillips, P.A. Williams & D.J. Wedlock. IRL Press, Oxford, UK, pp. 551–4.